Title

Interlaboratory Reproducibility of Contour Method Data Analysis and Residual Stress Calculation

Journal

Experimental Mechanics, 60(6)

ISSN

0014-4851

Authors

D'Elia, CR
Carlson, SS
Stanfield, ML
et al.

Publication Date

2020-07-01

DOI

10.1007/s11340-020-00599-0

Peer reviewed

Interlaboratory Reproducibility of Contour Method Data Analysis and Residual Stress Calculation

C.R. D'Elia[1], S.S. Carlson[2], M.L. Stanfield[2], M.B. Prime[3],
J. Araújo de Oliveira[4], T.J. Spradlin[5], J.B. Lévesque[6], M.R. Hill[1*]

[1] *Department of Mechanical and Aerospace Engineering, University of California, One Shields Avenue, Davis, CA 95616*
[2]*Southwest Research Institute (SwRI), 6220 Culebra Rd, San Antonio, TX 78238*
[3]*Los Alamos National Laboratory, Los Alamos, NM 87545*
[4]*StressMap, Engineering & Innovation, Open University, N2024, Venables Bldg. Walton Hall, Milton Keynes – MK7 6AA - UK*
[5]*United States Air Force, Air Force Research Laboratory, 2790 D. St. Wright-Patterson, AFB, OH 45433*
[6]*Hydro-Québec Research Institute, 1800, Lionel-Boulet, Varennes (Québec), Canada, J3X 1S1*

Submitted to Experimental Mechanics, November 15, 2019
Revised and Accepted April 29, 2020
Published online https://doi.org/10.1007/s11340-020-00599-0

ABSTRACT

Background: While the contour method for residual stress assessment has developed rapidly, no published study documents its interlaboratory reproducibility. Objective: Here we report an initial reproducibility experiment focused on contour method data analysis and residual stress calculation. Methods: The experiment uses surface topography data from a physical process simulation of elastic-plastic beam bending. The simulation provides surface topography, for input to the contour method data analysis, as well as a known residual stress field with 130 MPa peak magnitude. To increase realism, noise and specific artifacts are added to the topography data. A group of participants received the topography data (without the known residual stress), independently analyzed the data, and submitted results as a two-dimensional residual stress field. Results: Analysis of submissions provides a group average residual stress field and the spatial distribution of reproducibility standard deviation. The group average residual stress agrees with the known stress in magnitude and spatial trend. The reproducibility standard deviation ranges from 2 to 54 MPa over the measurement plane, with an average of 5.4 MPa. Reproducibility

* Corresponding Author, mrhill@ucdavis.edu, tel: +1-530-754-6178, fax: +1-530-752-4158

standard deviation is smaller in the cross-section interior (≤ 5 MPa), modest near local extrema in the stress field (5 to 10 MPa), and larger near the cross-section boundaries (10 to 30 MPa). The largest values of reproducibility standard deviation (up to 54 MPa) occur in limited areas where artifacts had been added to the topography data; while some participants identified and removed these artifacts, some did not, leading to systematic differences that elevated the standard deviation.

Keywords: contour method; residual stress; reproducibility; precision; uncertainty

1. INTRODUCTION

First published by Prime in 2001 [1], contour method experiments have been applied to quantify residual stress in a wide range of engineering applications. The method produces a two-dimensional (2D) map of the normal component of residual stress on a plane of interest. The method has high spatial resolution and can be applied to workpieces ranging in size from small coupons to full scale parts. The 2D map of residual stress normal to a plane of interest makes the method useful in fatigue and fracture assessments of airframe details and similar safety-critical structural elements. Current efforts are aimed to the quantify uncertainty and potential bias associated with residual stress data from the contour method.

Recent work on the contour method has established intralaboratory (within the same laboratory) repeatability [2] and a single measurement uncertainty estimator [3]; however, the interlaboratory reproducibility of the contour method has not been established. ASTM [4] defines a reproducibility condition as “conditions where test results are obtained with the same method on identical test items in different laboratories with different operators using different equipment”. The main objective of this paper is to describe a reproducibility experiment of

limited scope, being focused on specific steps of a contour method experiment: data analysis and residual stress calculation.

Performing the contour method reliably depends on sound procedures, good equipment, and experienced practitioners. The open literature provides resources and guidance for the contour method practitioner (e.g., [5,6]). A working group of recognized and published practitioners in the contour method was organized to support this reproducibility experiment. The group, and their total years of experience exercising the contour method, consists of:

- Dr. Mike Prime – Los Alamos National Laboratory – 20 years
- Dr. Michael R. Hill & Mr. Chris D'Elia – University of California – Davis – 19 years
- Dr. Jeferson Araujo de Oliveira – StressMap – 6 years
- Mr. Jean-Benoît Lévesque – Hydro-Québec Research Institute – 10 years
- Dr. T.J. Spradlin – United States Air Force – Air Force Research Laboratory (AFRL) – 5 years
- Dr. Scott Carlson – Southwest Research Institute (SwRI) – 4 years

At the outset of this work, this group agreed to describe and report results using randomly assigned codes to enable anonymity and promote open exchange; therefore, results here are attributed to "Lab X", where X is a randomly assigned integer ranging from 1 to 6.

2. METHODS

Contour method

The contour method is composed of five major steps [6]:

1. identifying a plane of interest in a part
2. cutting along the plane of interest to release residual stress
3. measurement of the topography of the cut surfaces
4. data processing of the surface topography (screening, aligning, filtering or smoothing, averaging), and
5. calculation of the residual stresses by linear elastic stress analysis

This first effort to assess contour method reproducibility is focused on steps 4 and 5, as the group considers them a significant potential source of error and uncertainty that has not been previously assessed.

During step 4, surface topography data from each half of the cut surface are processed to remove artifacts of measurement and outlying values, to align the two surfaces to a common coordinate frame, to average the surfaces together, and to smooth the topography to filter out roughness and measurement noise. The processed surface topography is then used as a displacement boundary condition in a linear elastic stress analysis, typically using finite element analysis (FEA). The calculated stress provides an estimate of the residual stress normal to the cut plane prior to making the cut [1,7].

In order to establish a representative and useful set of surface topography data for the present purposes, a process simulation was developed for elastic-plastic beam bending. An experimental apparatus for elastic-plastic bending, shown in Figure 1, was used by Prime in his seminal paper on the contour method [1], and is simulated herein. The surface displacements from the simulation provide a basis for the surface topography data supplied to the participants, and the residual stress from the simulation provides a benchmark to compare to calculated residual stress. Thus, the uncertainties associated with surface topography data processing are isolated from other uncertainty sources (e.g., those arising from cutting the part in half and measuring the topography).

Elastic-plastic simulation

The simulation of elastic-plastic four-point bending was developed using the commercial software ABAQUS [8]. The specimen was modeled as a three-dimensional solid. The geometry and boundary conditions used in the simulation are shown in Figure 2. The beam geometry has a

square cross-section of side length 31.75 mm near the ends and a smaller, rectangular gage section 12.7 mm wide and 31.75 mm high.

The bent bar was meshed using eight node hexahedral elements with incompatible modes (ABAQUS element type C3D8I). The boundary conditions were idealized as lines of prescribed constant displacements. The mesh was refined to ensure a converged solution, with the final mesh having nearly square elements 0.4 mm on each edge; in the gage section the mesh had 32 elements along the 12.7 mm width, 80 elements along the 31.75 mm height with 80 elements along the 31.75 mm gage length.

The material assumed in the simulation is Aluminum 7075-T651. This material differs from that used earlier by Prime but is consistent with future work of the present authors. The heat treatment T651 was chosen due to the availability of full stress strain curves in the literature. The elastic properties are Young's modulus E = 71,000 MPa and Poisson's ratio v = 0.33 [9]. Plasticity follows a nonlinear kinematic hardening model with a Mises yield surface. The kinematic hardening component is composed of a linear Ziegler hardening law and a recall term. For uniaxial loading, the hardening law for the kinematic backstress parameter, α, is

$$\dot{\alpha} = C\frac{1}{\sigma|_0}(\sigma - \alpha)\dot{\bar{\varepsilon}}^{pl} - \gamma\alpha\dot{\bar{\varepsilon}}^{pl} \qquad \text{Eqn (1)}$$

where C is the initial kinematic hardening modulus, $\sigma|_0$ defines the size of the yield surface at zero plastic strain, $\dot{\bar{\varepsilon}}^{pl}$ is the equivalent plastic strain rate, and γ is the rate at which the kinematic hardening modulus decreases with increasing plastic deformation [10,11]. The hardening law constants were calibrated with half-cycle stress-strain data from a tension test (using Figure 3.7.8.1.6(p) of [9]), which yielded: C = 3,496,353 MPa; $\sigma|_0$ = 513,873 MPa; γ = 26.433.

The simulation was executed in three steps: loading, unloading, and cutting. The maximum applied displacement of the central rollers during the bending was 1.21 mm, which provided adequate plastic deformation and residual stress at the center section of the bar. The cut was modeled as an interaction model change where a geometric region was deactivated and the remaining material was allowed to relax. The process step sequence is evident in the contour plots of Figure 3. The residual stress condition follows unloading (Figure 3(b)) and the surface topography was taken as the change in surface displacement between the residual stress condition and the relaxed condition after the cut (Figure 3(c)).

Two sets of simulation output data are used in subsequent steps to assess interlaboratory reproducibility. The first set of data is values of stress normal to the cut plane, at nodes on the cut plane, following unloading and prior to the cut. This set of stress values was retained as *benchmark* residual stress data. The second set of data is values of post-cut displacement normal to the cut plane, at nodes on the cut plane, following cutting. This set of displacement values is used to establish *surface topography input data* for contour method analysis and calculations. Typical contour analysis includes assessment of data from both sides of the cut, and so the simulation displacements were replicated to provide two (initially identical) sets of cut surface topography data. For both sets, surface topography height was linearly interpolated onto a fine grid, having in-plane spacing of 0.1 mm (in the range of typical contour method practice). Artifacts were added to each set of topography data that represented a coordinate measuring machine (CMM) probe tip reading off the edges of the sample. The interpolated out-of-plane displacements were modified along the left and right edges at X = 0 mm and X = 12.70 mm. Along these edges, the data between Y = 16.16 mm and Y = 27.03 mm were removed and replaced with a linear segment interpolated along the Y direction. Random noise was then added

to all values of out-of-plane displacement, with the noise drawn from a normal distribution having zero mean and 0.3 μm standard deviation. Surface topography data were saved in two text files, one file for each side of the cut (side 1 and side 2), with each file having 39,344 lines of triples, each triple having two values of in-plane position and one value of out-of-plane height.

Roles and Procedures

During the course of this work, roles were assigned to participating individuals and procedures developed to maintain study integrity. One person was assigned the role of *simulator* (co-author Stanfield). The simulator developed and executed the simulation described above, keeping private all details of the material model and the benchmark residual stress data. Another person was assigned the role of *captain* (co-author Carlson). The captain worked together with the simulator to establish a well-defined *problem statement* to be provided to the larger group of *participants* (all co-authors except Stanfield). Each participant received the problem statement, including surface topography data and performed their own data analysis and residual stress calculation. After a defined work period (roughly six weeks), each participant submitted an estimate of residual stress to the captain. To ensure independent residual stress estimates, during the work period participants were prohibited from contacting one another; side-discussions were avoided by routing participant questions to the captain, who relayed the questions and responses to all participants. After the work period, the captain anonymized each participant submission with an integer code (to disguise its origin). The set of submissions was then assessed by the *analyst* (co-authors D'Elia and Hill, working together). To perform a useful analysis, the analyst was given access to the benchmark residual stress field. A summary of the analyst assessment was then provided to the entire *team* (all co-authors) and discussed at length. This paper conveys the findings of the team.

Problem Statement

The data analysis and residual stress calculation problem statement contained a description of the geometry of the part (similar to Figure 2), the coordinate system used to define the cut surface topography, elastic material properties (identical to those used in the simulation), and surface topography data. Surface topography data were provided to participants in the form of (X, Y, Z) triples, where X and Y locate a point on the contour plane, and Z provides the surface height. Participants were not required to perform any coordinate transformations, interpolations, or further manipulations to the topography data.

The problem statement asked participants to submit values of residual stress normal to the cutting plane on a regular rectangular grid with 0.32 mm spacing (41 points across the 12.7 mm width and 101 points along the 31.75 mm height).

Documentation of Practice

A questionnaire was used following the period of work to document methods employed by each participant. Specific questions addressed three main themes: topography screening, topography smoothing or fitting, and residual stress computation (i.e., finite element stress analysis). Examples of specific questions asked are: whether and how outliers were identified and processed; the type of smoothing or fitting used to generate stress analysis inputs; certain details regarding the stress analysis, including number and type of elements. The responses to the questionnaire are included below and are useful for documenting common practices.

Analysis of Submissions

Color contour maps as well as vertical and horizontal line plots are used to compare each submission to the benchmark residual stress. Plots use linear interpolation of submitted data when required. Stress differences (submitted stress minus benchmark) are also assessed. Contour

maps of stress differences identify areas of the submitted 2D stress maps where they deviate from the benchmark residual stress. For each submission the root mean square (RMS) of stress difference values (at all in-plane positions) provides a single metric to gage agreement between the submission and the benchmark. Pointwise mean and standard deviation were computed across all submissions to assess accuracy (mean versus benchmark) and reproducibility (standard deviation).

3. RESULTS

The surface topography data provided to the participants contains measurement noise and artifacts superimposed on the simulation displacements, as shown in Figure 4. The peak-to-valley range of the data is approximately 20 μm and the simulated surface noise is consistent with the specified 0.3 μm standard deviation. The signal to noise ratio is approximately 10. Although similar, the Side 1 and Side 2 surface topography data are unique due to differences in the added noise. The three-dimensional plots, Figure 4a and b, indicate a dominant topography variation along the Y direction, consistent with the bending simulation. The elevation views, Figure 4c and d, show curvature along the Y direction near local extrema at approximately Y = 7.5 mm and 25.0 mm. The CMM artifacts are most apparent in Figure 4a and b between Y = 20.0 mm and 25.0 mm. The CMM artifacts reach about 3 μm in these regions.

The displacement data from the finite element simulation are plotted in Figure 5 along a vertical line at X = 6.35mm and a horizontal line at Y = 25.4mm. Data provided to the participants is also shown in Figure 5 including points within ± 0.05 mm of the two lines to illustrate the noise in the topography data.

Results from the participant questionnaire are tabulated for different areas of inquiry. Basic attributes of topography screening are summarized in Table 1, which shows that only one of the

six participants did not remove points from the provided surface topography data. Among those that did remove points, only one used a statistical method for doing so; the remaining participants used a manual method to identify and remove points.

The surface data processing methods used by the participants are summarized in Table 2. Of the six participants, five used a variant of splines to fit the averaged displacement surface. Of those five, three used a B-spline for fitting the surface, and two used an unspecified type of spline fitting method. One participant utilized what was described as a "discontinuous analytical function" to fit the surface.

The displacement boundary conditions calculated by each participant are plotted in Figure 6 along a vertical line at X = 6.35 mm (Figure 6a) and a horizontal line at Y = 25.4mm (Figure 6b). The relatively small differences reported between the participants are shown by closer examination along the vertical centerline for $7 \leq Y \leq 10$ mm (Figure 6c). The results show varying levels of smoothness, with most being smooth but results from Lab 5 having short range fluctuations. Relative to others, Labs 3 and 6 report large gradients near some of the plane boundaries (Figure 6b, near X = 0 for Lab 3 and near X = 12.7 mm for Lab 3 and Lab 6).

Residual stress calculation methods used by participants are summarized in Table 3. Most participants used the ABAQUS software package and one participant used a Fortran-based program. The participants used general purpose brick elements, some using linear displacement interpolation (C3D8, C3D8R) and others quadratic (C3D20, C3D20R). The number of elements used by each participant varied by a factor of 14, with a lower element count for those using quadratic elements.

Color map plots of residual stress returned by each participant are shown in Figure 7 along with the benchmark (Figure 7g). The fields are all nearly one-dimensional, being approximately

uniform along the X direction and varying along the Y direction. These are consistent with the elastic-plastic bending process and the benchmark stress state. All the results are similar in overall trend, including the general locations of the peak tensile and compressive stresses as well as the general locations of the local extrema.

Additional details are evident in the stress differences (submission – benchmark) of Figure 8. Within the core of the coupon the largest differences between the benchmark and each submission are reported within approximately 3.0 mm of the local extrema (near Y = 7.5 mm and 25 mm). Large differences of residual stress are reported by Lab 3 and Lab 6 near locations where the CMM artifacts were introduced in the surface topography data. These locations are near the edges at X = 0 and 12.7 mm, and for $17 \leq Y \leq 27$ mm. These elevated stress differences occur near both edges (X = 0 and 12.7 mm) for Lab 3 but near only one edge for Lab 6 (X = 12.7 mm).

The single-value difference metrics, RMS difference and maximum difference, for each participant are compared graphically in Figure 9 and further, statistics of the stress differences are summarized in Table 4. Half of the participants, Lab 1, Lab 2, and Lab 4 reported stresses with lower RMS and max differences than the other participants. These participants had RMS difference over the cross-section of 2 to 3 MPa, which is low compared to the 130 MPa peak residual stress magnitude; RMS difference for others was somewhat higher at 10 to 15 MPa. The lowest RMS stress difference was 2.1 MPa (Lab 1 and Lab 2) and the largest was 15.4 MPa (Lab 5). Maximum pointwise differences were 5 to 10 times larger than the RMS average differences. The two highest maximum differences were 116 MPa (Lab 3) and 119 MPa (Lab 6).

The mean residual stress field and reproducibility standard deviation, computed from all the participants, is given in Figure 10 along with the benchmark stress field. Overall, the mean

residual stress field in Figure 10b is similar to the benchmark stress field in Figure 10a, having local tensile and compressive extrema along the Y dimension. The reproducibility standard deviation is relatively low over much of the cross-section, less than 5 MPa, but is higher in some areas. The highest standard deviations (> 25 MPa) are in localized areas that correspond to regions where Labs 3 and 6 had larger stress differences but other Labs did not: near the edges at X = 0 and 12.7 mm and for $17 \leq Y \leq 27$ mm. The standard deviation is also higher, 15 to 22 MPa, near the edge at Y = 0. Comparatively, moderate standard deviations of 5 to 15 MPa are present in a 6 mm band centered near 5 and 26 mm, near the local extrema in the benchmark stress field.

Line plots in Figure 11 provide residual stress along two specific trajectories, one at the mid-width (X = 6.35 mm) and another near the compressive peak of the residual stress field (Y = 25.4 mm). The benchmark and the average participant residual stress are compared in Figure 11a and b, with error bars indicating the standard deviation. Differences between each participant stress field and the benchmark are plotted in Figure 11c and d. Results plotted along Y in Figure 11a show clearly the higher standard deviations of approximately 5 to 15 MPa near the local stress extrema and at the free edges (Y = 0 and 32 mm) and the lower standard deviations elsewhere. Results plotted along X near the compressive stress inflection in Figure 11b show that standard deviation is 3 to 10 MPa for most points but is as large as 50 MPa near the edges (X = 0 and 12.7 mm). Stress differences along the Y direction in Figure 11c show that Lab 5 has larger stress differences, which elevate standard deviation. Stress differences along the X direction in Figure 11d show the large differences for Lab 3 (near X = 0 and X = 12.7 mm) and Lab 6 (near X = 12.7 mm). These large differences create the high standard deviations of nearly 50 MPa in these localized areas.

A further set of plots in Figure 12 show more clearly results at the left and right edges, X = 0.0 mm and X = 12.7 mm. The areas affected by the CMM artifacts, 17 mm ≤ Y ≤ 27 mm, exhibit high standard deviation in Figure 12a and b. The stress differences of Figure 11c show the outlying character of the stress differences at X = 0 mm for Lab 3; similarly, the stress differences of Figure 11d show the outlying character of the stress differences at X = 12.7 mm for both Lab 3 and Lab 6.

4. DISCUSSION

As the contour method matures and is used for more applications, understanding the uncertainty associated with the calculated residual stress is essential. Many applications, including aerospace, demand statistically-derived allowable parameters, thus requiring residual stress inputs to be characterized statistically. Processing the raw surface topography data and computing residual stresses (via an elastic stress analysis) represent critical steps in the contour method process that may introduce associated uncertainty. This work determined the spatial distribution of reproducibility standard deviation through a round robin effort among expert practitioners.

Overall, the participant residual stress submissions agree with one another but vary in two distinct ways: the amount of small length scale variation, and the stresses reported near the CMM artifacts. The differences in small length scale variation are most apparent in the line plots of Figure 6 and Figure 11 and to a lesser degree in the stress color map of Figure 7. The surface displacements (Figure 6) and residual stress (Figure 11) are smooth for all participants but those for Lab 5 have small length scale variations (note that the peaks and valleys in the stress distribution and displacement are coupled because the displacements are the main input to the residual stress calculation). The surface data processing performed by Lab 5 had lower inherent

smoothing than the processing performed by the other participants. Large residual stress differences, up to 116 MPa, are evident in results for Labs 3 and 6 near locations of the CMM artifacts as shown in Figure 12 (as well as in Figure 11d near X = 0 and 12.7 mm). These stress differences are consistent with the displacements for Labs 3 and 6 in Figure 6 which show a sharp trend toward lower displacement at X = 0 and 12.7 mm for Lab 3 and at X = 12.7 mm for Lab 6. The questionnaire responses confirm that Lab 3 did not remove outlying topography data (Table 1); the displacements of Figure 6 suggest that Lab 6 removed outlying data near X = 0 but did not remove the similar outlying data near X = 12.7. All participants but Lab 3 and 6 removed the outlying data and obtained residual stress closer to the benchmark, as shown by stress differences near zero in Figure 12c and d. Labs 3 and 6 did not remove the outlying data and obtain larger localized stresses near the CMM artifacts. These larger stresses pull the group average away from the benchmark and elevate the reproducibility standard deviation. These effects of outlying topography data are noteworthy and underscore the importance of carefully examining the underlying data in order to identify and remove outliers and artifacts before smoothing and computing residual stress. These examinations and subsequent outlier removals are critical decisions made by the human operator and can significantly influence the resulting stress calculations.

Care was needed when the analyst assessed participant submissions and performed summary analyses. Interpolation and transformation were needed because some participants provided results at FEA nodal locations rather than at the grid points requested in the problem statement. The points in the contour maps of residual stress in Figure 7 and stress difference in Figure 8 reflect the positions of the data submitted by each participant. Computing the stress differences in Figure 8 required interpolating the benchmark stress to locations used in each submission. All

line plots use data interpolated to the requested regular grid with 0.32 mm spacing. In most areas, effects of interpolations are negligible; however, the effects of interpolation are more significant in areas close to steep, near-edge gradients reported by some labs. Care was taken to ensure that the points raised in this paper are robust to, and not unduly influenced by, the specific details of interpolation and other features of the data analyses.

It is important to note that this round robin activity required participants to deviate from their typical contour method workflows. Each participant was provided with background information (e.g., coordinate frame, geometry, elastic properties), surface topography data, and instructions for reporting computed residual stress, which is different from each participant executing a contour method measurement from start to finish under their typical procedures. Situational factors in this, or any, round robin process can lead to results that are less representative of each practitioner's typical workflow. For example, most participants perform smoothing and filtering using data acquired from conventional tactile or laser profilometer tools. Surface roughness and measurement noise in typical measurements can be larger (~10 μm peak to peak) than was assumed here (~2 μm peak to peak, which is about 6 times the 0.3 μm RMS added noise), and larger noise could lead to different reproducibility standard deviation. The CMM artifacts of this study are another situational factor: a practitioner working with their typical topography measurement equipment would inspect for and remove such artifacts; but, in this study some identified the artifacts and removed them while others did not, and this factor had a notable effect on the outcomes obtained.

Reproducibility standard deviation varies spatially, as shown clearly in Figure 10c, Figure 11 and Figure 12. Higher values occur near extrema, at edges, and near the CMM artifacts. These features are specific to the part geometry (i.e., contour plane boundaries and edges), potential

errors in metrology (e.g., noise level, introduction of artifacts), and the underlying residual stress field (i.e., stress level, stress gradients). In a physical experiment, they would also be influenced by aspects of the cut. While the present work addresses a simple geometry (rectangular section) and residual stress state (varying mainly along one direction), it does illustrate useful features that may arise commonly in other parts (e.g., higher reproducibility standard deviation near extrema and edges). The potential for elevated uncertainty near surfaces and extrema is important in the context of engineered residual stress fields that put high compressive residual stresses at fatigue prone surfaces. When it is important to explicitly manage reproducibility, such as in a high-performance environment, reproducibility should be characterized in full field on representative test pieces rather than by assuming representative levels of uncertainty.

Values of interlaboratory reproducibility standard deviation found here are similar to the levels of *intralaboratory* repeatability [2] and uncertainty found by Olson et al [12,13] in the context of physical contour method measurements. They studied a range of residual stress bearing sample types, in a range of metals, and found that repeatability standard deviation and uncertainty were lower in the part interior and higher at the contour plane boundaries. They found representative contour method uncertainty divided by elastic modulus of approximately 125 parts-per-million (ppm) in the interior and 250 ppm near (within 1 mm of) the contour plane boundaries. Using the value of modulus provided above, gives representative uncertainty of 9 MPa on the interior and 18 MPa on the edges, which are similar to the values of interlaboratory reproducibility found here.

The present authors are committed to additional work that assesses contour method reproducibility. Physical experiments are planned in which each participant performs the cutting through stress calculation steps of the contour method, described above as steps 2 through 5.

5. CONCLUSIONS

This paper reports reproducibility standard deviation for contour method residual stress data established by an experiment of limited scope with reported reproducibility standard deviation specific to two steps of the contour method measurement: surface topography data analysis and residual stress calculation. A single analyst performed a physical process simulation of elastic-plastic beam bending and then sectioning typical of the contour method. The analyst then provided a set of surface topography data to a team of 6 participants who worked in isolation to determine residual stress on the contour plane. All participants in the round robin reported residual stress values that were similar to a known benchmark, being largely one-dimensional and consistent with elastic-plastic bending. The average of all the residual stress submissions agrees well with the benchmark stress state and finite element simulation. The reproducibility standard deviation quantifies dispersion among the 6 participants and varies with position in the contour plane. Relative to the 130 MPa peak residual stress magnitude, the reproducibility standard deviation is low (< 5 MPa) over much of the cross section, higher (15-22 MPa) near the cross-section boundaries, and moderate (5-15 MPa) near the local extrema in residual stress. Large (up to 54 MPa) reproducibility standard deviation occurred in isolated regions where topography artifacts were introduced into the input data and were handled differently by different participants (some removed them, and some did not).

6. COMPLIANCE WITH ETHICAL STANDARDS

This study was performed by the authors without the support of external funding.

Disclosure of potential conflicts of interest

- SSC, MLS, TJS, and JBL report no potential conflicts of interest.
- CRD is a graduate student pursuing a doctorate under the guidance of MRH.

- MBP holds patent US6470756B1 on the contour method, from which modest royalties are received.
- JAO and MRH have separate economic interests in contour method measurements that derive from their employment by (JAO) or an ownership interest in (MRH, Hill Engineering, LLC of Rancho Cordova, CA, USA) a firm providing contour method measurements.

All authors affirm that these potential conflicts of interest did not play a significant role in the work reported here and that this paper reflects the consensus of all authors.

REFERENCES

[1] Prime, M.B. Cross-Sectional Mapping of Residual Stresses by Measuring the Surface Contour after a Cut. J. Eng. Mater. Tech. 123: 162 168, 2001;

[2] Hill, M.R., Olson, M.D. Repeatability of the Contour Method for Residual Stress Measurement. Exp. Mech. 54, 7 1269 – 1277, 2014.

[3] Olson, M.D., DeWald, A.T., Prime, M.B., Hill, M.R. Estimation of Uncertainty for Contour Method Residual Stress Measurements. Exp. Mech. 55, 3, 577 – 585, 2014.

[4] ASTM E691-15, Standard Practice for Conducting an Interlaboratory Study to Determine the Precision of a Test Method, 2015, ASTM International, West Conshohocken, MA

[5] Hosseinzadeh, F., Kowal, J., Bourchard, P.J. Towards Good Practice Guidelines for the Contour Method of Residual Stress Measurement. J. Eng. 8, 453 – 468, 2014.

[6] Prime, M.B., DeWald, A.T. The Contour Method. In: Schajer, G.S., ed. *Practical Residual Stress Measurement Methods*, West Sussex John Wiley & Sons West Sussex: 2013.

[7] Prime, M.B., Gonzales, A.R. Contour Method: Simple 2-D Mapping of Residual Stresses. In: *Proceedings of the 6th International Conference on Residual Stresses*, IOM Communications, London: 617 – 624, 2000.

[8] Dassault Systèmes Simulia Corp., ABAQUS Analysis User's Guide version 6.14, Providence, RI, USA, 2014.

[9] Metallic Materials Properties Development and Standardization (MMPDS): MMPDS-06. United States Federal Aviation Administration, Washington D.C., 2011.

[10] Alberto Franchi, Paolo Riva, Francesco Genna, Incremental elastic-Ziegler kinematic hardening plasticity formulations and an algorithm for the numerical integration with an "a priori" error control, In D. E. Grierson et al. (eds.), Progress in Structural Engineering, 407-421. (1991)

[11] Dassault Systèmes Simulia Corp., ABAQUS Analysis User's Guide version 6.14, section 23.2.2, Models for metals subjected to cyclic loading, Providence, RI, USA, 2014.

[12] Olson, M.D., DeWald, A.T., Hill, M.R. Validation of a Contour Method Single-Measurement Uncertainty Estimator, Exp. Mech. 58, 767-781, 2018. https://doi.org/10.1007/s11340-018-0385-4

[13] Olson, M.D., DeWald, A.T., and Hill, M.R., Repeatability of Contour Method Residual Stress Measurements for a Range of Materials, Processes, and Geometries, Materials Performance and Characterization 7(4), 427-445, 2018. https://doi.org/10.1520/MPC20170044

TABLES

Participant	Artifacts Identified	Artifact Handling	Method
1	Yes	Deleted	Manually
2	Yes	Deleted	Manually
3	No	N/A	N/A
4	Yes	Deleted	Manually
5	Yes	Deleted	Modified Thompson Tau Method
6	Yes	Deleted	Manually

Table 1 – Summary of participant responses to questions regarding data processing

Participant	Type of fitting used	Optimization of Solution in Stress or Displacement	Metric for Optimizing Solution
1	Splines	Stress	Estimated average uncertainty in the stresses1
2	Splines	Both displacement and stress are considered in developing an optimal result.	Global and local metrics for misfit of displacements and the smoothness of the stress field are considered
3	Splines	Both	RMS convergence in displacement vs. Actual and convergence of mean, maximum, and minimum stress
4	Discontinuous Analytical Function	Stress	Consistency of stress line profiles at varying smoothing levels
5	B-Splines	Displacement	Minimizing RMS of Residual Between Fit and Displacements
6	B-Splines	Stress	Estimated average uncertainty in the stresses[1]

Table 2 – Summary of participant responses to questions regarding topography smoothing or fitting

[1] The average uncertainty for a given spline fit (i.e. knot density) is basically the standard deviation between those stresses and the stresses given by other spline fits with slightly higher and lower knot densities.

Participant	Software used	Element type	Number of elements
1	Abaqus	C3D20R	50,000
2	Abaqus	C3D8	91,600
3	Fortan-based Program	8 Node Linear	140,440
4	Abaqus	C3D20R	86,964
5	Abaqus	C3D8-Incompatible	440,748
6	Abaqus	C3D8	727,272

Table 3 – Summary of participant responses to questions regarding residual stress calculation

Participant	Number of Points	RMS Average Difference (MPa)	Max Difference (MPa)
1	3141	2.1	18.9
2	1071	2.1	15.7
3	4141	11.5	116.5
4	12281	3.1	24.5
5	680	15.4	44.0
6	4515	9.8	119.2

Table 4 – Statistical information for stress differences for each participant

FIGURES

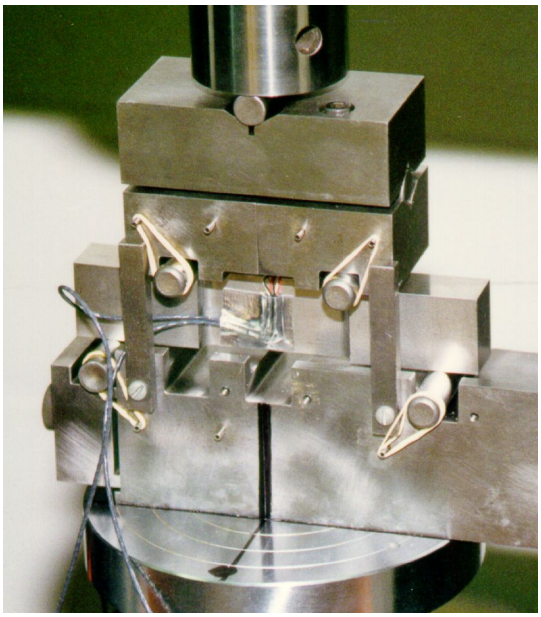

Figure 1 – Specimen and bending fixture used in 2001 four-point bend experiments performed by Prime [1]

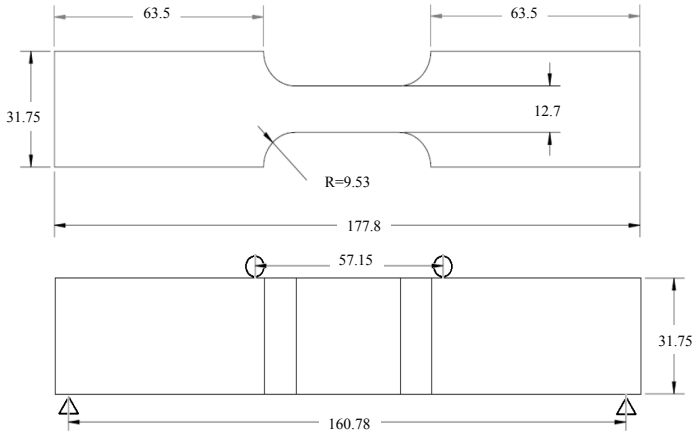

Figure 2 – Four-point bend geometry and boundary conditions (dimensions in mm)

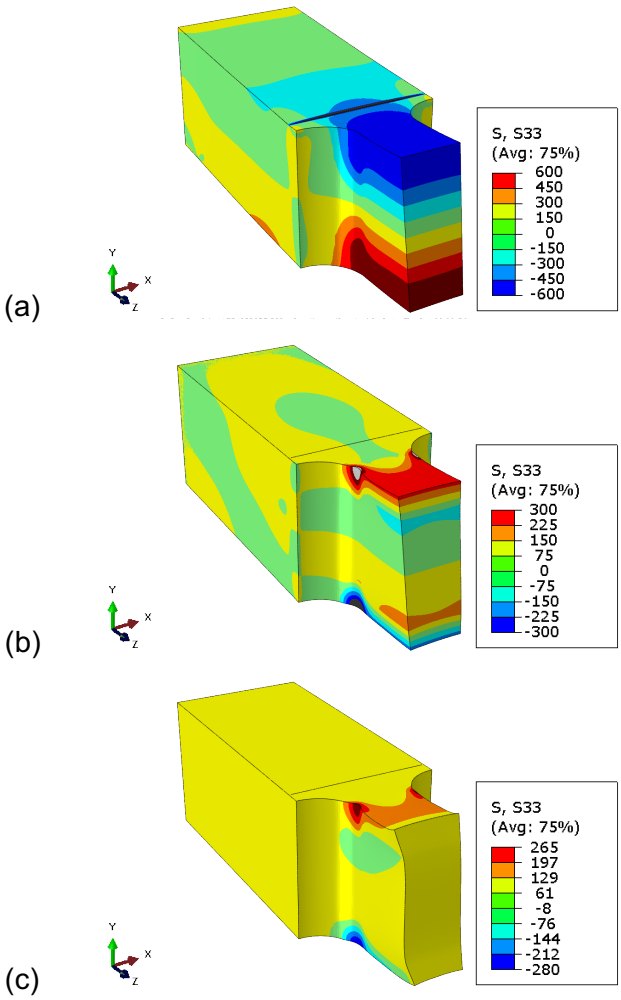

Figure 3 – Contour plots of σ_{zz} (in MPa) from the simulation: (a) at maximum deflection, (b) after unloading (residual stress condition), and (c) after the cut (cut condition)

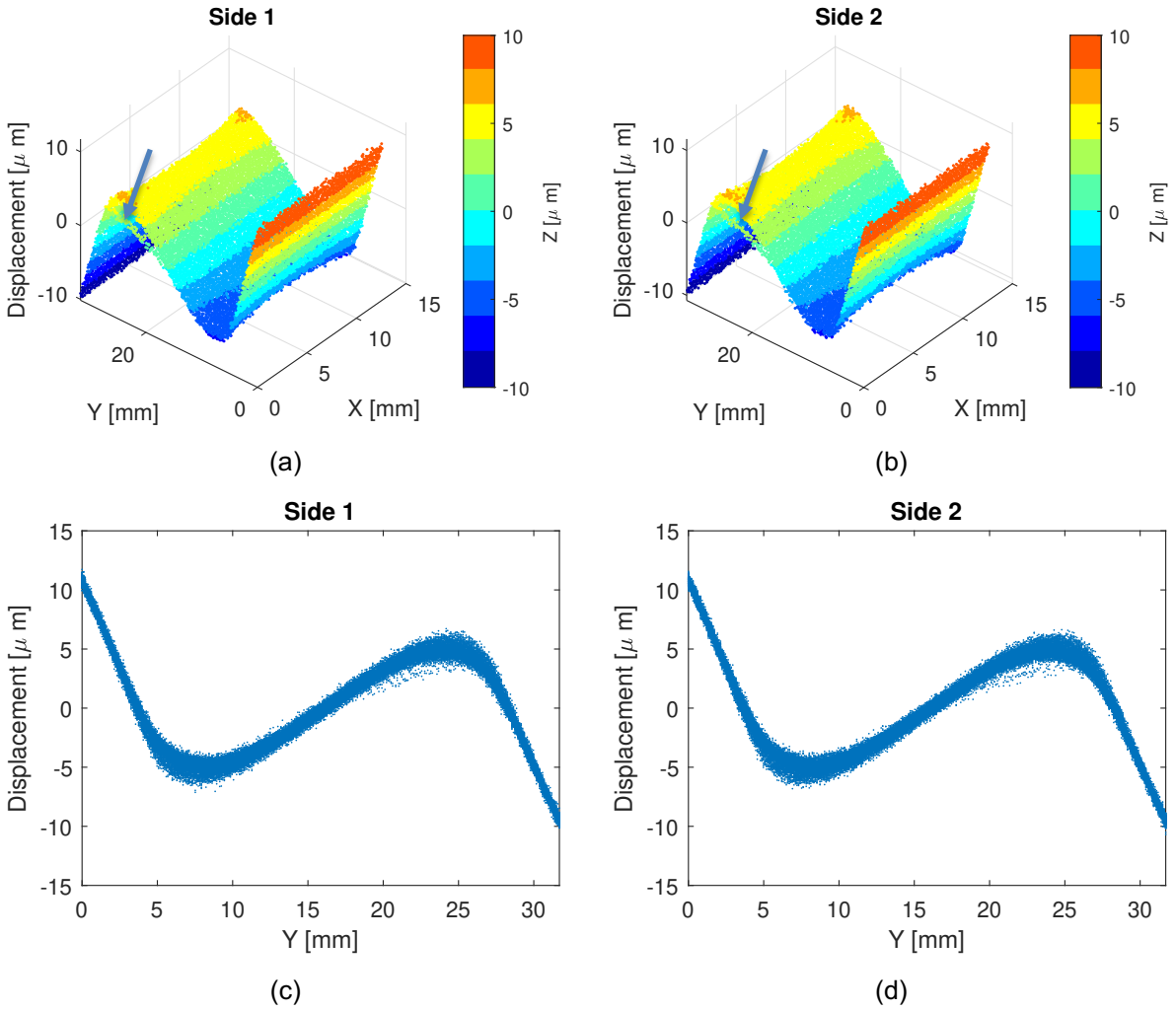

Figure 4 – Surface topography data provided with the problem statement in perspective view for (a) side 1, (b) side 2, and in a side view for (c) side 1 and (d) side 2. Arrows in (a) and (b) indicate added artifacts

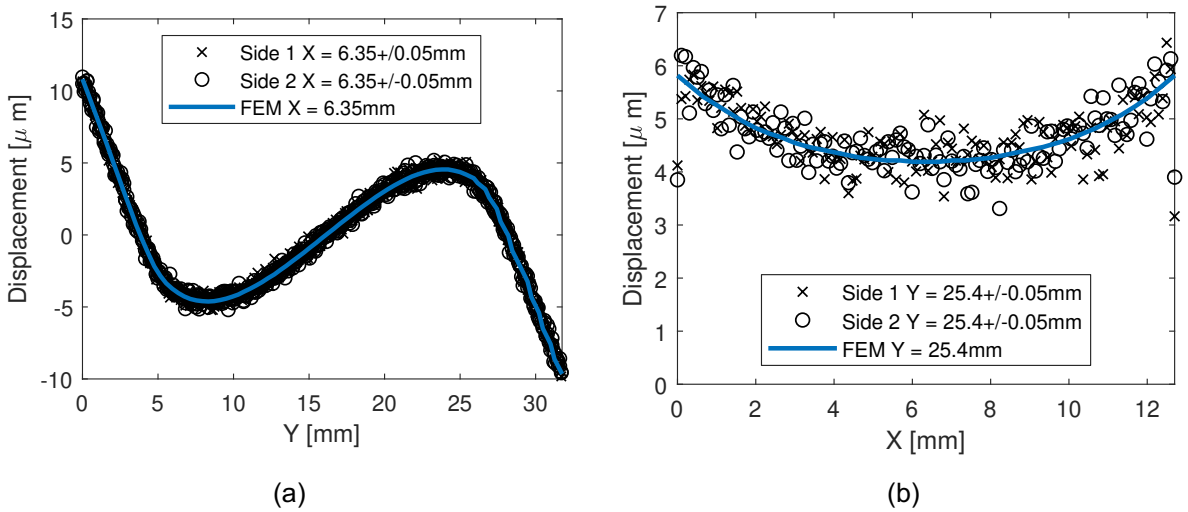

Figure 5 – Surface topography data provided with the problem statement plotted with underlying FEM displacements

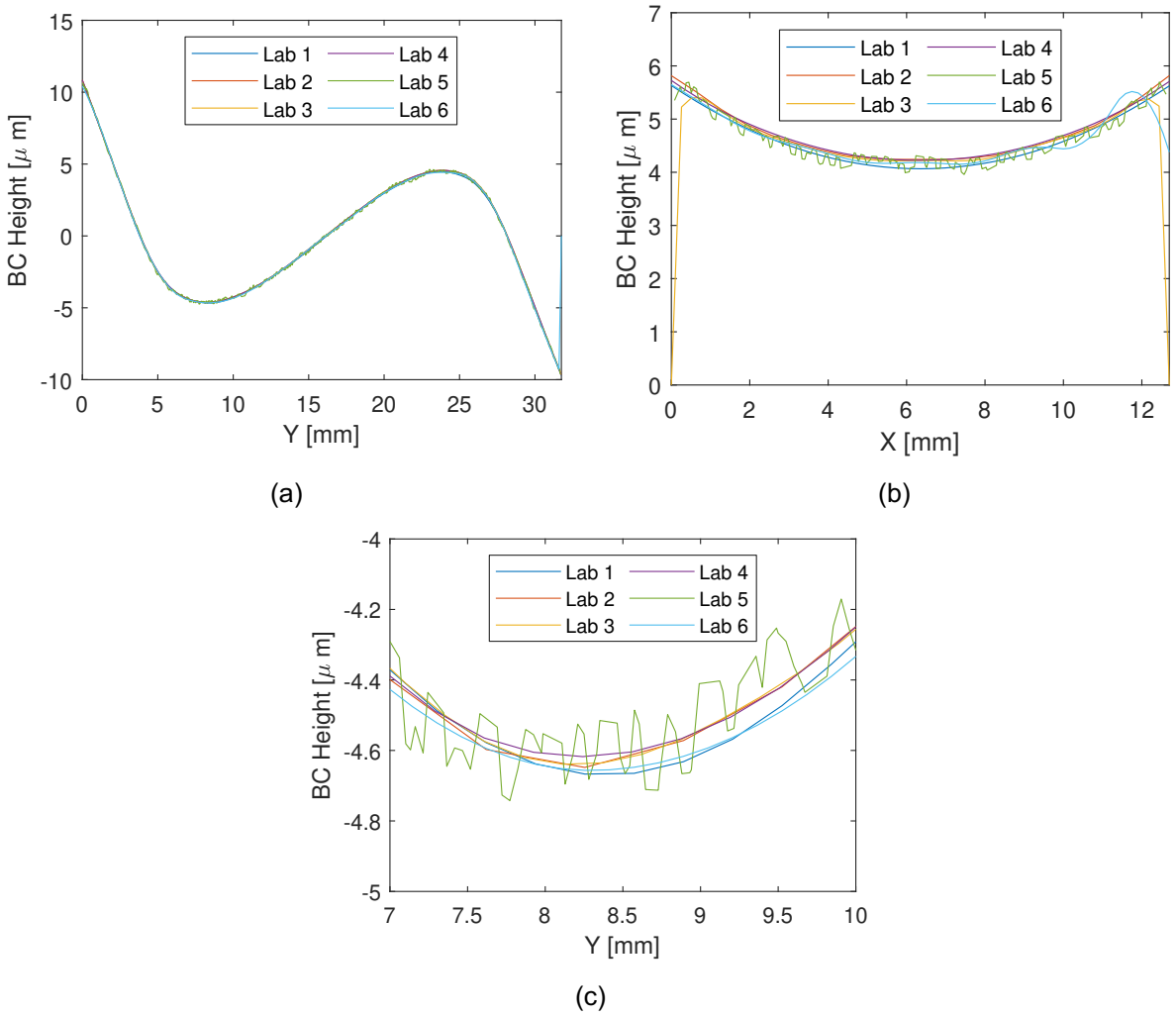

Figure 6 – Participant boundary conditions used in finite element stress calculation shown along (a) the vertical centerline, X=6.35 mm, (b) near stress local extrema, Y=25.4 mm, with (c) a magnified view for 7 ≤ Y < 10 mm along the vertical centerline, X = 6.35 mm

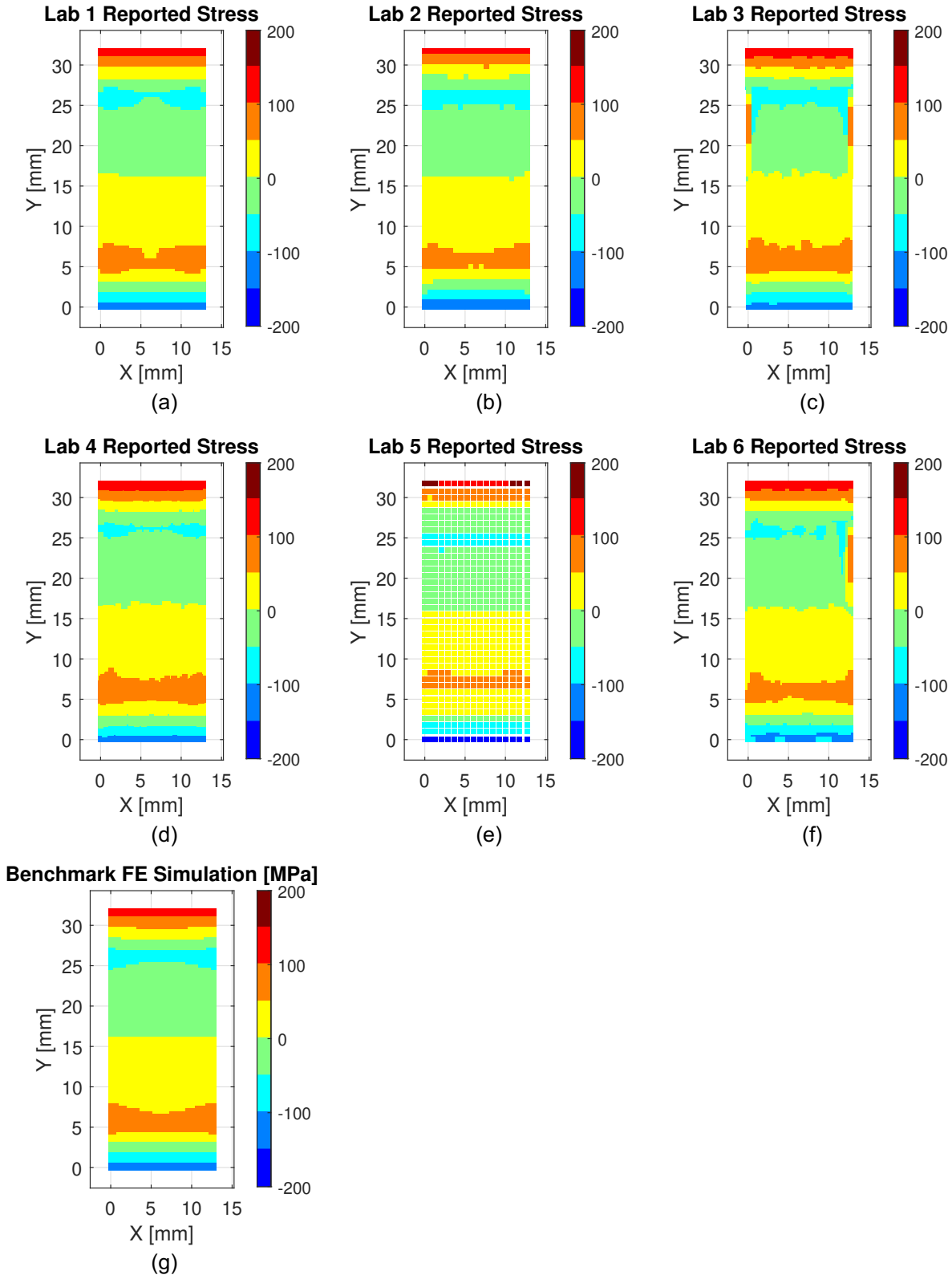

Figure 7 – Contour plots of residual stress submitted by each participant and benchmark finite element simulation. Differences in the contour plot appearance reflect the point spacing of the data provided by each participant. The data provided by each participant are summarized in Table 3.

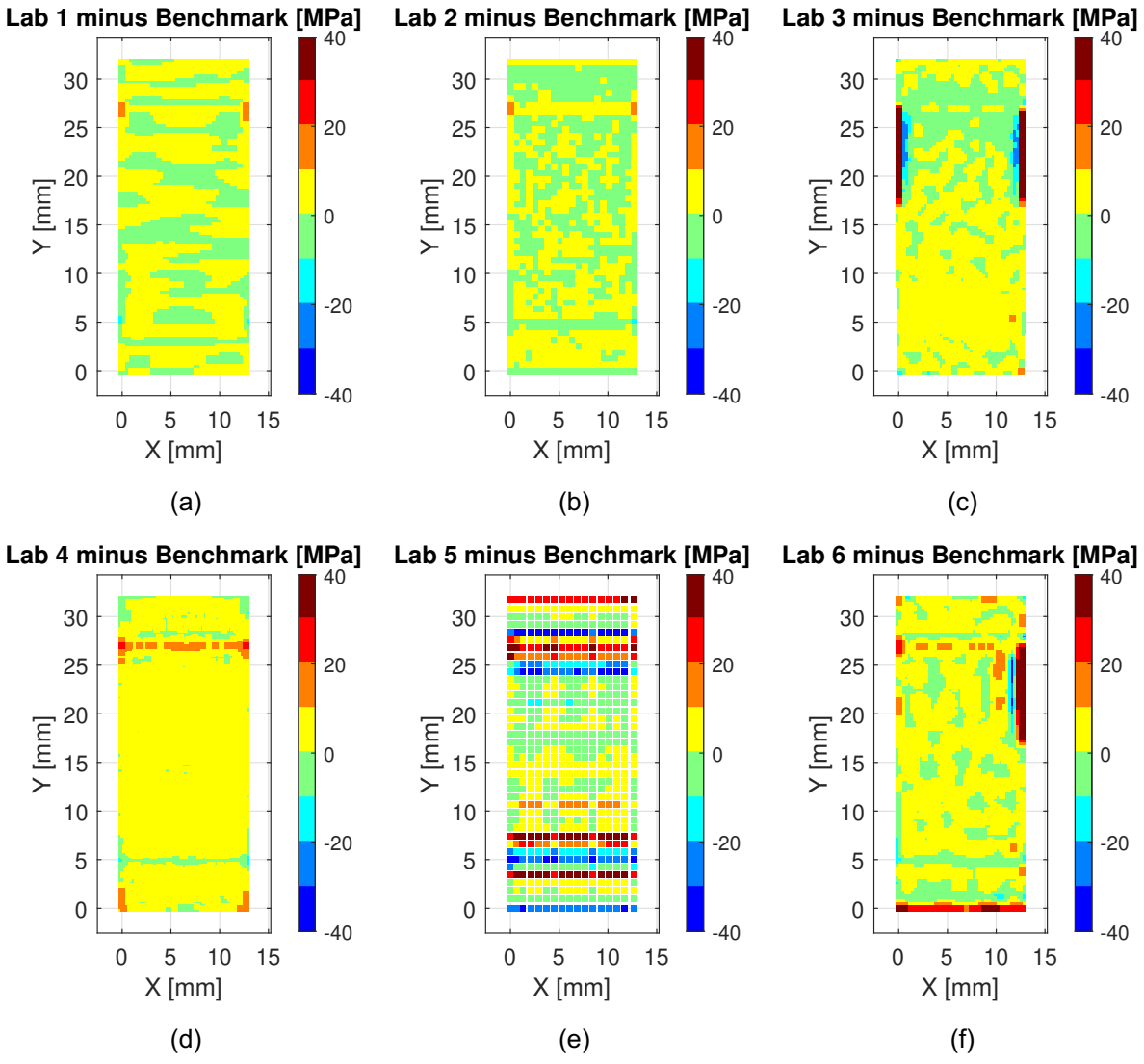

Figure 8 – Contour plots of the difference between submitted stress and benchmark for each participant

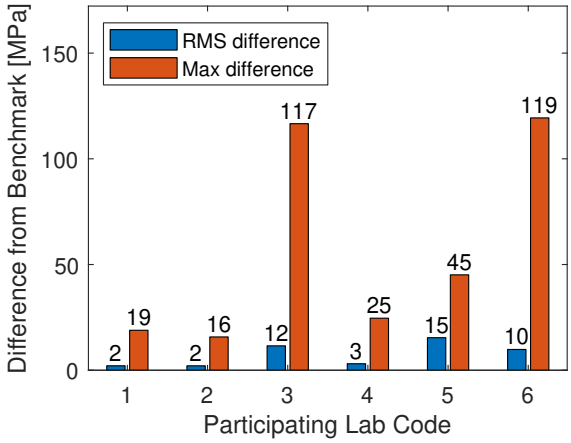

Figure 9 – RMS and max difference from benchmark finite element solution.

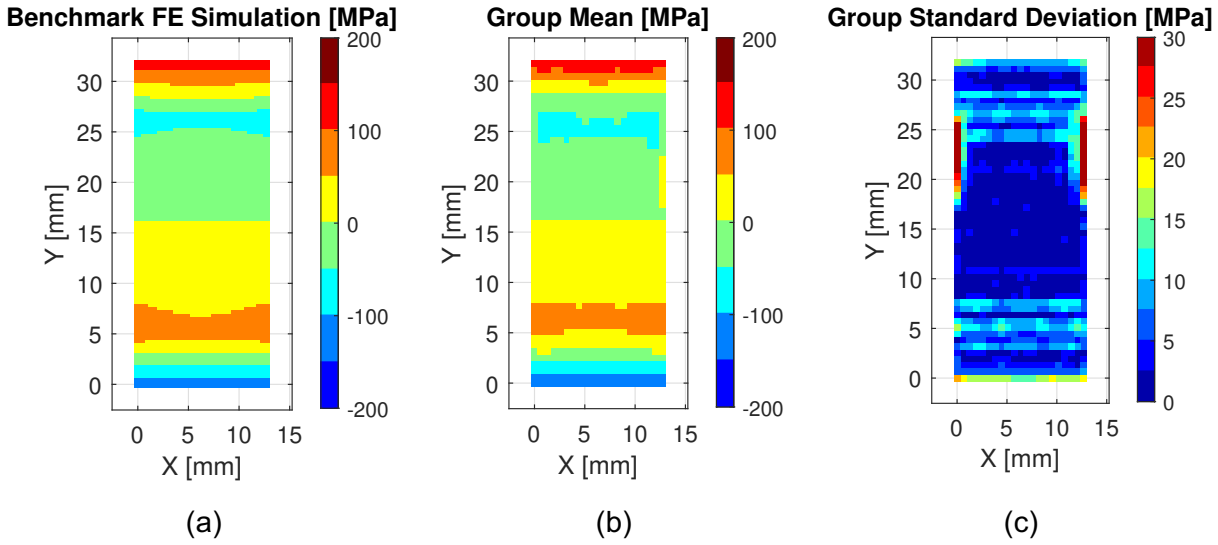

Figure 10 – Maps of (a) the benchmark residual stress, (b) the group mean residual stress, and (c) the reproducibility standard deviation

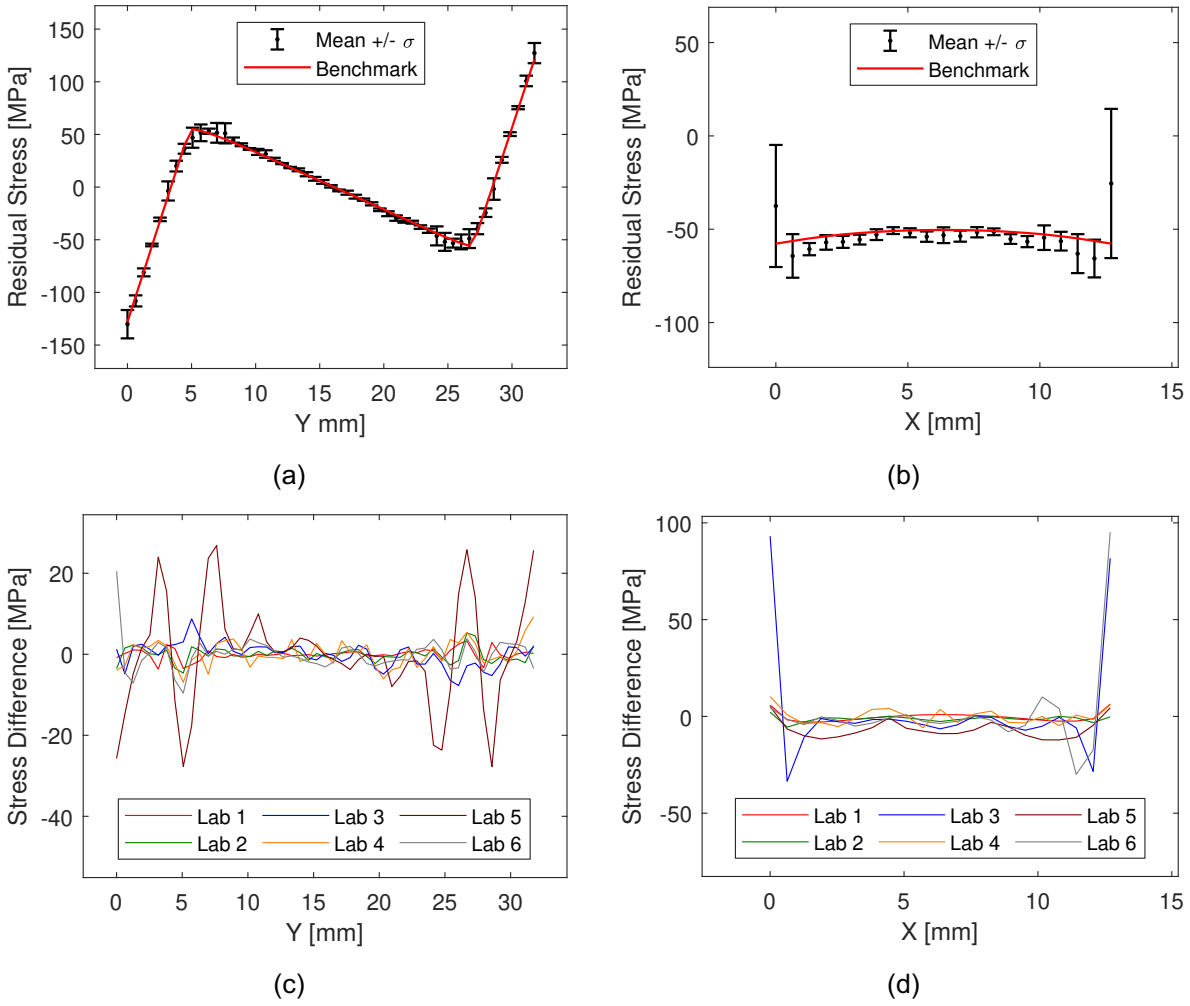

Figure 11 – Line plots of group mean and benchmark with error bars indicating reproducibility standard deviation along (a) X = center and (b) Y = 25.4 mm; (c) and (d) show individual stress differences along the same lines

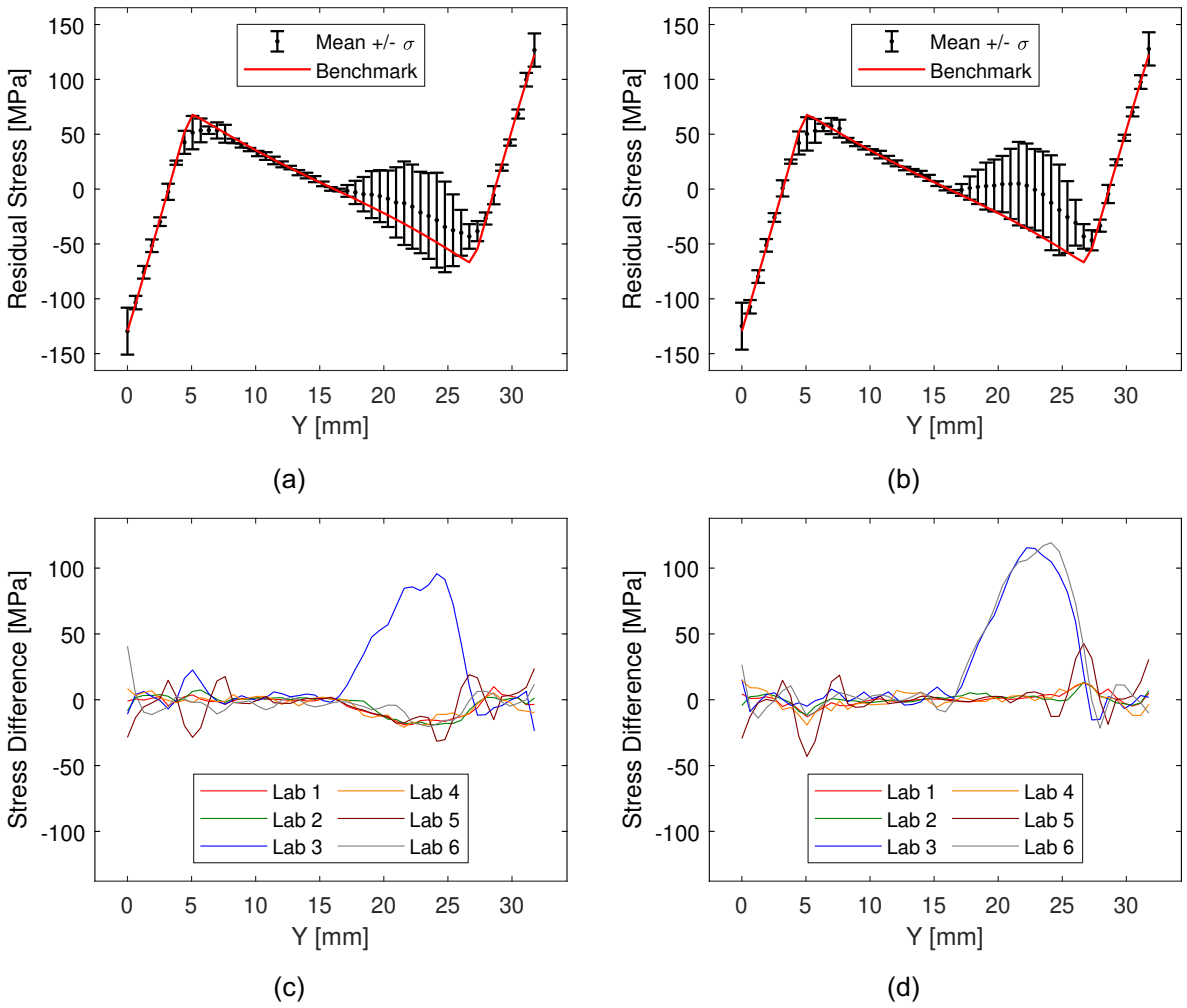

Figure 12 – Line plots of group mean and benchmark with error bars indicating reproducibility standard deviation along the cross-section boundaries at (a) X = 0 and (b) X = 12.7 mm; (c) and (d) show individual stress differences along the same lines